Biochemical and Biophysical Research Communications 409 (2011) 22–27

Contents lists available at ScienceDirect

Biochemical and Biophysical Research Communications

journal homepage: www.elsevier.com/locate/ybbrc

Cu/Zn superoxide dismutase is differentially regulated in *period* gene-mutant mice

Yeong-Su Jang, Myung-Han Lee, Sang-Hyuk Lee, Kiho Bae *

Division of Biological Science and Technology, Yonsei University, Wonju 220-710, Republic of Korea

ARTICLE INFO

Article history:
Received 19 April 2011
Available online 28 April 2011

Keywords:
Cu/Zn superoxide dismutase
Circadian rhythm
Period
Oxidative stress
tert-Butylhydroperoxide

ABSTRACT

The circadian clock in the brain coordinates the phase of peripheral oscillators that regulate tissue-specific physiological outputs. Here we report that circadian variations in the expression and activity of Cu/Zn superoxide dismutase (SOD1; EC 1.15.1.1) are present in liver homogenates from mice. The *SOD1* mRNA expression from wild-type (WT) mice peaked at *Zeitgeber Time* 9 (ZT9; 9 h after lights-on time). While there was no rhythmicity in that from *period*2 (*per*2) gene knockout (P2K) mice, the level of *SOD1* from *per*1/*per*2 double knockout (DKO) mice was significantly elevated at ZT5. The enzyme activity of SOD1 was also rhythmic in the mouse liver. Moreover, the total amount of the SOD1 exhibited a rhythmic oscillation with a peak at ZT9 in the liver from WT mice. We also found that *tert*-butylhydroperoxide (*t*-BHP)-induced oxidative damage in both WT and P2K mouse embryonic fibroblast (MEF) cells resulted in the up-regulation of SOD1 levels. Our data suggest that the expression of an important antioxidant enzyme, SOD1, is under circadian clock control and that mice are more susceptible to oxidative stress depending on the time of day.

1. Introduction

In nearly all organisms, physiological and behavioral processes exhibit approximately 24 h rhythms that are controlled by a circadian clock. These rhythms are fundamental biological systems in most organisms. In mammals, the master clock is located in the suprachiasmatic nucleus (SCN) at the ventral end of the hypothalamus [1]. The SCN controls neural and humoral signals that drive output rhythms to synchronize the peripheral clock with day/night cycles. Environmental time cues such as light and temperature are known to play roles in continuously resetting the rhythm of the clock [2,3]. The purpose of studying the circadian rhythm is to identify how *in vivo* physiological changes take place in a beneficial direction by recognizing and responding to external environmental changes.

It was first discovered that changes in the behavior of fruit flies were caused by a *per* gene mutation in the 1970s. Clock genes such as *timeless*, *dClock*, *cycle*, *doubletime* and *cryptochrome* were also later identified in fruit flies [4–6]. A mouse with a *clock* gene mutation was the first mutation obtained in mammals. Since then, our knowledge of the mammalian clock system has progressed rapidly and many gene knockout studies in mice have been performed. More recently, expression patterns of circadian clock genes have been compared in the head and body of *Drosophila* and the SCN, fibroblast and liver in mammals through DNA chip technology. It is well established that biological clock genes are expressed in the SCN as well as in the liver, muscle, and kidneys [7–9]. Peripheral clocks reside in each organ and ensure that organ-specific metabolism is regulated properly according to time.

Organisms are exposed to various forms of oxidative stresses, such as light exposure during the day, including UV light, and the formation of reactive oxygen species (ROS) caused by feeding and locomotion. For instance, harmful UV radiation particularly affects the skin and eyes and triggers the formation of ROS, and the resulting oxidative stresses generally induce apoptosis. Therefore, intracellular ROS or reactive nitrogen species (RNS) should be regulated very precisely, as any misregulation can cause aging and degenerative diseases [10,11]. An antioxidant enzyme, SOD1, which is encoded by a so-called 'ancient gene' [12,13], is known to remove superoxide. Endogenous circadian and exogenously driven daily rhythms of antioxidant enzyme activities have been described in several phylogenetically distant organisms. Substantial amplitudes detected in several cases suggest the significance of rhythmicity in avoiding excessive oxidative stress [14]. Previous studies have shown that there are circadian variations in the SOD enzyme activity in livers from Balb/c mice [15] and in the level of mRNA for *Cu/Zn SOD* in the rat medial basal hypothalamus [16]. Thus, it appears organisms actively use circadian rhythms in order to cope with threats of oxidative stresses.

Considering the significance of the countermeasures for oxidative stress relating to the circadian clock, there are surprisingly few studies on the time-dependent regulation of antioxidant enzymes in mammals. Therefore, we investigated whether the

* Corresponding author. Address: Division of Biological Science and Technology, Yonsei University, 1 Yonseidae-gil, Wonju 220-710, Republic of Korea. Fax: +82 33 760 2183.
E-mail address: kbae@yonsei.ac.kr (K. Bae).

0006-291X/$ - see front matter © 2011 Elsevier Inc. All rights reserved.
doi:10.1016/j.bbrc.2011.04.099

expression of the antioxidant enzyme, SOD1, has circadian variations according to oxidative stress, and we also examined the impact of pro-oxidant treatment on the expression of this enzyme. We used *per* gene mutant mice and were indeed able to identify a close relationship between SOD1 expression, oxidative stress, and the functioning of the circadian clock.

2. Material and methods

2.1. Animals

Male 129/sv strains of 7–9-week-old mice were housed under a 12 h light:12 h dark schedule (LD cycles; lights on at 0700 h) and fed *ad libitum*. The *per*-mutant mice used in this study have been described previously [17], and were maintained in the animal facility of Yonsei University at Wonju, Korea. All animal care and procedures were in accordance with the guidelines of the Institutional Animal Care and Use Committee. All mice were synchronized with LD cycles over two weeks and 3–5 male mice were sacrificed by cervical dislocation for each experiment.

2.2. Preparation of cDNA and real time polymerase chain reaction (PCR)

Liver tissues were isolated from mice sacrificed at 4 h intervals starting at 0700 h. Total RNA from each sample was extracted using TRI reagent (Sigma, St. Louis, MO, USA), following the manufacturer's instructions. Tissue samples in 1 ml of TRI reagent per 50–100 mg of tissue were homogenized using a motorized, handheld homogenizer. The amount of RNA was quantified by spectrophotometry, and the integrity of RNA was confirmed by agarose gel electrophoresis. Any contaminating genomic DNA was eliminated using the RNase-Free DNase Kit (Promega, Madison, WI, USA). The PrimeScript 1st strand cDNA Synthesis Kit (TaKaRa, Dalian, China) was used to synthesize cDNA from 1 μg of total RNA, according to the manufacturer's protocol. The *β-actin* housekeeping gene was used as a constitutive control for normalization. The following primer pairs were used:

SOD1, forward, 5′-GATGAAGAGAGGCATGTTGGA-3′
reverse, 5′-TGTACGGCCAATGATGGAATG-3′;
β-actin, forward, 5′-TTTTCCAGCCTTCCTTCTTGGG-3′
reverse, 5′-TGTGTTGGCATAGAGGTCTTTACGG -3′.

PCR were carried out using the StepOnePlus Systems (Applied Biosystems, Foster City, CA, USA). PCR conditions included one cycle of 10 min at 95 °C followed by 35 cycles of 15 s at 95 °C, 30 s at 65 °C, and 30 s at 72 °C. Detection of fluorescent product was carried out at the end of the 72 °C extension period. The amount of cDNA in each sample was calculated by the $2^{-\Delta\Delta Ct}$ method [18]. All samples were analyzed in triplicate and in three independent measures.

2.3. Western blotting

Proteins were extracted in lysis solutions with 20 mM HEPES (pH 7.5), 100 mM KCl, 5% glycerol, 5 mM EDTA (pH 8), 1 mM $MgCl_2$, 1 mM DTT, 0.1% Triton X-100, and protease inhibitor cocktail tablets (Roche Diagnostics, Indianapolis, IN, USA). Protein extracts of 20 μg each were boiled for 5 min at 95 °C in sodium dodecyl sulfate (SDS)-sample buffer, loaded onto a 12% polyacrylamide gel and then separated by SDS–polyacrylamide gel electrophoresis (PAGE). Protein bands were transferred to nitrocellulose membranes (Bio-Rad, Hercules, CA, USA) and stained briefly with

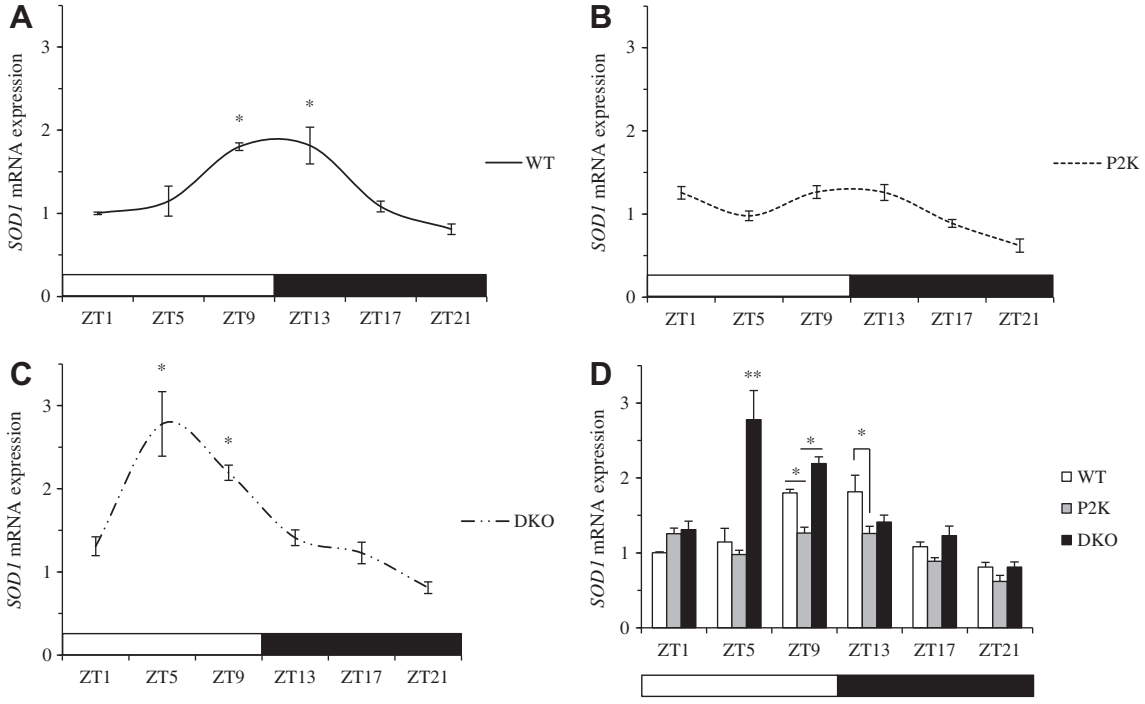

Fig. 1. Daily rhythms of *SOD1* mRNA expression in the mouse liver. Mice were entrained to standard LD cycles and liver tissues were collected at the times indicated in figure, and cDNAs were prepared from liver extracts. Shown are the results of real-time PCR analysis of *SOD1* expression. The housekeeping gene, *β-actin*, was used as a gel loading control for normalization. (A) *SOD1* mRNA levels are rhythmic in the liver from WT mice (shown as a line graph). (B) *SOD1* mRNA levels are reduced in the liver from P2K mice (as a broken line). (C) *SOD1* mRNA levels are phase-shifted in the liver from DKO mice (as a broken line with two dots). (D) Temporal profiles of *SOD1* mRNA levels in the liver of WT (open bar), P2K (gray bar), and DKO (filled bar) mice are depicted in a histogram. The open and filled bars on the *X*-axis of graphs A–C and below the graph in D represent 12 h of daytime and 12 h of darkness, respectively. Each data point represents the mean ± SEM of three samples. Statistical analysis was performed by Student's *t*-test; *denotes the difference between two genotypes and **denotes the difference among three genotypes, each with statistical significance at $P < 0.05$.

Ponceau S (Sigma, St. Louis, MO, USA) to confirm equal loading. Membranes were then blocked in 5% nonfat dry milk (Bio-Rad, Hercules, CA, USA) in Tris-buffered saline with 0.05% Tween-20 (TBST) for 1 h at room temperature. Membranes were subsequently probed with anti-Actin goat polyclonal antibodies (1:5000 dilution, Santa Cruz, CA, USA) and anti-SOD1 rabbit polyclonal antibodies (1:5000 dilution, Santa Cruz, CA, USA) diluted in TBST with 5% blocking solution. Following incubation with the appropriate secondary antibodies, immunoblots were developed using Western blot detection reagents (Amersham, Buckinghamshire, UK) and exposed to X-ray film according to the manufacturer's protocol.

2.4. Enzyme activity assay

The activity of SOD1 in liver homogenates was determined using an SOD1 Enzyme Assay Kit (EMD/Calbiochem, La Jolla, CA, USA). Cytosolic fractions of liver were prepared in homogenization solutions containing 20 mM HEPES (pH 7.2), 1 mM EGTA, 210 mM mannitol, and 70 mM sucrose, followed by centrifugation at 10,000*g* for 15 min at 4 °C. The SOD activity assay utilizes the reduction of tetrazolium salt by xanthine oxidase-generated superoxide radicals. The assay was performed in a 96-well plate and the absorbance was measured at 450 nm using a 96-well plate reader (VersaMax, Molecular Devices, Sunnyvale, CA, USA) in triplicate.

2.5. Cell culture, t-BHP treatment, and measurement of cell viability

MEF cells were grown in Dulbecco's Modified Eagle's Medium (DMEM) supplemented with 10% fetal bovine serum (FBS, GIBCO, Carlsbad, CA, USA) at 37 °C under 5% CO_2. To measure the cell viability, MEF cells were seeded onto six-well plates and treated with various *t*-BHP concentrations (10–500 μM) for 12 h. Cells were then incubated in methylthiazole tetrazolium (MTT) solutions and the absorbance was measured in an ELISA plate reader at 590 nm. Each assay was repeated three times, using three wells per drug concentration in each experiment.

Approximately 5×10^5 cells/Petri dish (10 cm in diameter) were also plated five days before the experiment. The cells were cultured in a serum-rich medium (DMEM supplemented with 50% horse serum [GIBCO, Carlsbad, CA, USA)]) for 2 h. The medium was then replaced with DMEM without serum. MEF cells were treated with various concentrations (10–500 μM) of a pro-oxidant (*t*-BHP) for 12 h, and the amount of SOD1 in these cells was measured by immunoblotting.

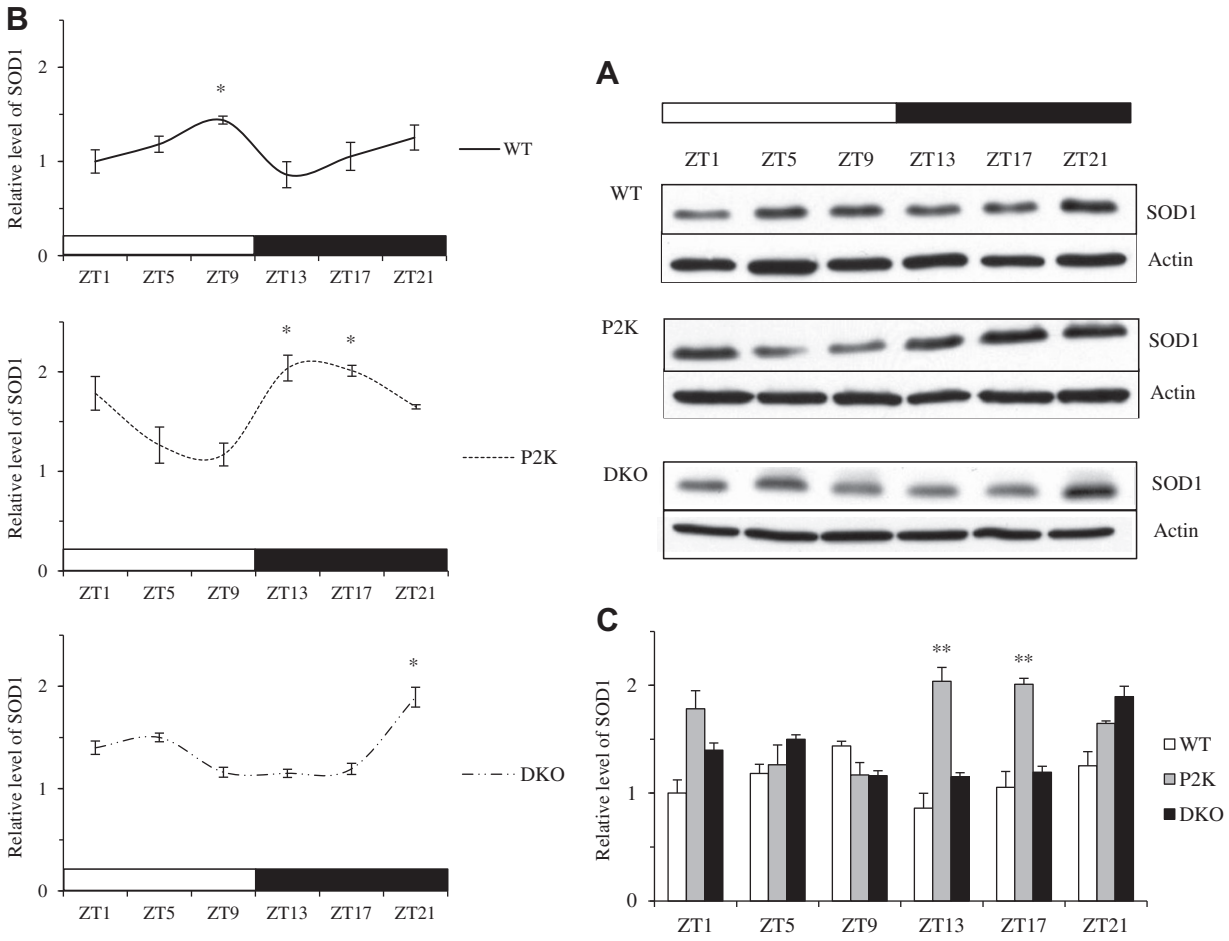

Fig. 2. Rhythmic variation of SOD1 in the mouse liver. Liver samples prepared from WT, P2K, and DKO mice (the same as those in Fig. 1) were used for protein extract preparation. Immunoblotting was performed on liver extracts collected at ZT1 to ZT21. (A) Representative gel images are shown. The housekeeping protein, *β-actin*, was used as the internal loading control for normalization. The intensity of the SOD1 band from each gel shown in (A) was determined by densitometry, and temporal profiles of SOD1 expression in the liver from WT (top), P2K (middle), and DKO (bottom) mice are depicted as individual line graphs (B) and are also summarized as a histogram (C). The open and filled bars above the blot in A and on the *X*-axis of graphs in B represent 12 h of daytime and 12 h of darkness, respectively. The line marks in B are the same as those described in the Fig. 1 legend. Values are expressed as mean ± SEM, and $n = 3$–4 for each time point. *denotes the peak level of SOD1 expression in each genotype and **denotes the difference among three genotypes, each with statistical significance at $P < 0.05$.

3. Results

3.1. SOD1 mRNA levels are altered differentially in circadian clock mutant mice

First, we measured the temporal expression of *SOD1* mRNA in mouse liver tissue by quantitative RT-PCR. As shown in Fig. 1A, WT mice exhibited a robust rhythmicity in *SOD1* mRNA levels, with low levels from ZT21 to 1 and peak levels from ZT9 to 13. The level of *SOD1* mRNA expression from P2K mice exhibited little or no change across time points and was lower than that of WT mice (Fig. 1B). Interestingly, in DKO mice, we observed a shift in the phase of *SOD1* expression. The phase of *SOD1* mRNA expression in DKO mice advanced about 4 h when compared to that of WT mice. Indeed, the expression of *SOD1* in DKO mice was already high in midday with a peak from ZT5 to 9 (Fig. 1C). We found a significant difference in *SOD1* expression among genotypes, especially from ZT5 to ZT13.

3.2. Expression of SOD1 is under circadian regulation in the mouse liver

Next, we measured the total amount of SOD1 during LD cycles in the mouse livers by Western blot analysis (Fig. 2A). In WT mice, SOD1 protein was at its maximum at ZT9 (Fig. 2B top left). The total protein level shifted in P2K mice, with peak levels at ZT13 to 17 (Fig. 2B middle left). Interestingly, the rhythmic expression of SOD1 in DKO mice peaked at ZT21 and reached a trough between ZT9 and 13, that is, the phase was delayed about 12 h compared to that of WT mice (Fig. 2B bottom left). It was evident that there is a phase difference in the peak level of SOD1 expression among genotypes (Fig. 2C).

3.3. Temporal profile of SOD1 enzyme activity in the mouse liver

The enzyme activity of SOD1 in cytosolic fractions of livers from WT, P2K and DKO mice was analyzed at different times during the day. There was an oscillation in the WT liver: the enzyme activity peaked at ZT9 and troughed at ZT21 (Fig. 3A). The P2K liver also exhibited a weak rhythmicity in SOD1 activity, with a peak around ZT13. However, the enzyme activity of SOD1 in P2K liver was weaker than that in the WT liver and was phase-shifted about 4 h (Fig. 3B). The SOD1 enzyme activity in DKO mice was the highest, peaking at ZT5 (Fig. 3C). Overall, SOD1 activity was clearly different among genotypes and time-of-day specific (Fig. 3D).

3.4. t-BHP-induced oxidative damage in MEF cells

We observed that cell viability was significantly reduced when *t*-BHP-induced oxidative stress was applied to MEF cells, as determined by MTT assays. Exposure of the MEF cells to *t*-BHP caused a dose-dependent decrease in cell viability. As illustrated in Fig. 4A, 12 h treatment of *t*-BHP at a concentration of 50 μM led to a significant reduction in cell viability. WT MEF cells that were exposed to 250 and 500 μM *t*-BHP manifested a decrease in viability. Oxidative stress induced by *t*-BHP also resulted in dramatic changes in P2K and DKO MEF cells. While the viability of WT MEF cells decreased in a dose-dependent manner, that of P2K and DKO cells began to drop drastically starting at 250 μM *t*-BHP.

To further examine *t*-BHP-induced oxidative damage in MEF cells, SOD1 expression in cells initially exposed to 10–500 μM of *t*-BHP for 12 h was determined (Fig. 4B). Both WT and P2K MEF cells were found to have a progressive and dose-dependent increase in SOD1 expression. Interestingly, SOD1 in DKO MEF cells maintained a high and constant level independent of *t*-BHP dose (Fig. 4C).

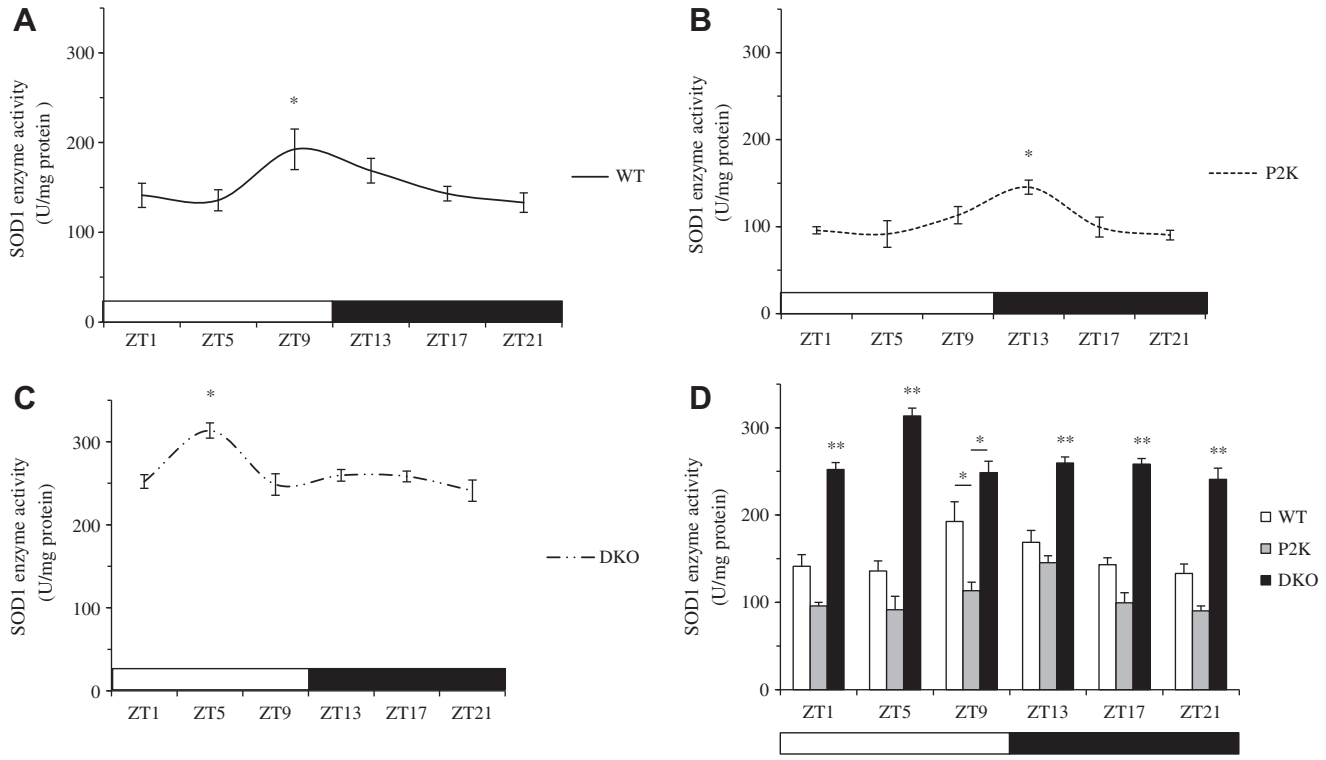

Fig. 3. Rhythmicity of SOD1 enzyme activity in the mouse liver. Cytosolic fractions of liver were prepared by homogenization, and the enzyme activity of SOD1 was measured as described in the materials and methods section. The SOD1 activity oscillated in the liver extracts from WT (A), P2K (B) and DKO (C) mice, and had specific peak values for each genotype (*). (D) Temporal profiles of SOD1 enzyme activity in the liver of WT, P2K and DKO mice are depicted in the histogram. The line marks are the same as those described in the Figs. 1 and 2 legend. Each data point represents the mean ± SEM of three samples [Student's *t*-test, * and **, $P < 0.05$].

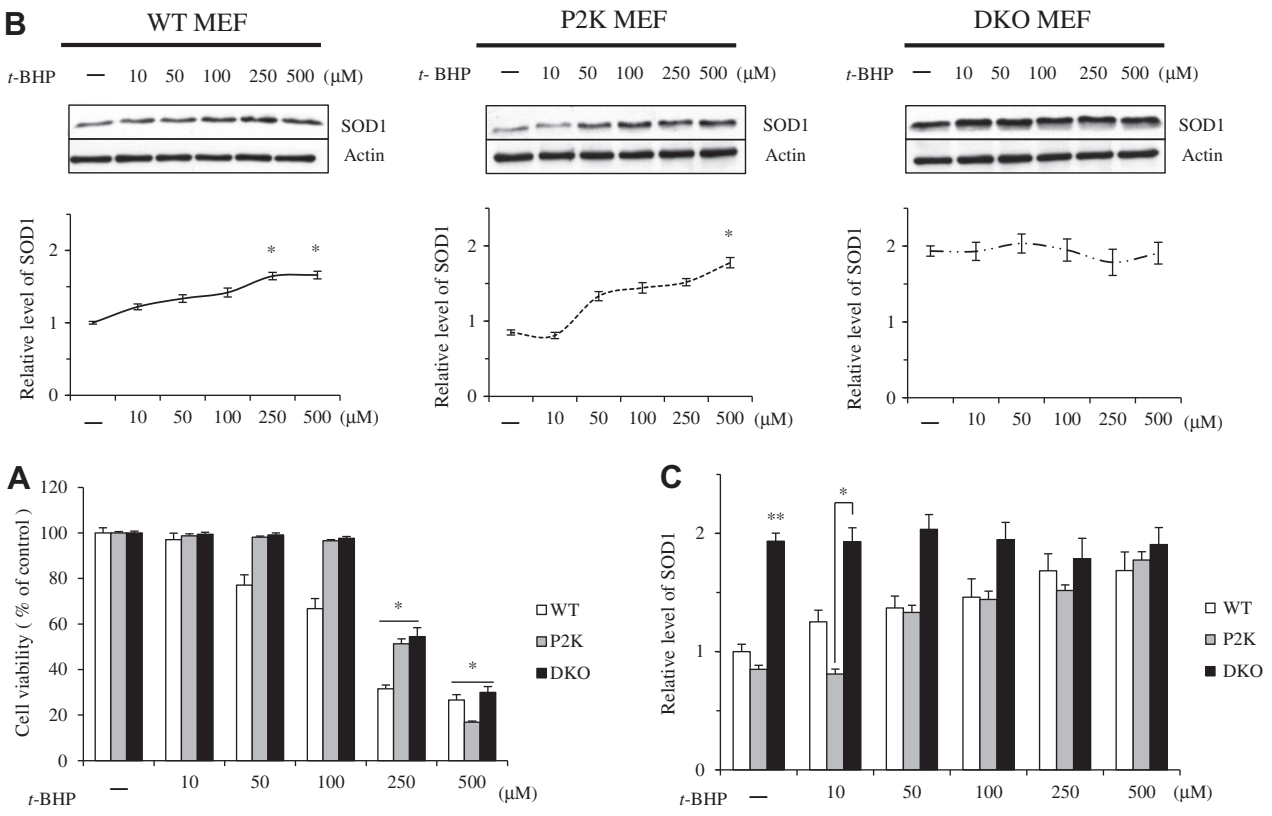

Fig. 4. Effects of *t*-BHP on SOD1 expression in MEF cells. (A) Cell viability following a 12-h exposure to *t*-BHP is depicted in the histogram. MEF cell lines of three different genetic backgrounds were exposed to increasing concentrations (10–500 μM) of *t*-BHP for 12 h and the extent of cell death was determined by MTT assays. (B) Three MEF cell lines were treated with various concentrations (10–500 μM) of *t*-BHP for 12 h and the effects of *t*-BHP treatment were detected by immunoblotting. The housekeeping protein, β-actin, was used as the internal loading control. The relative level of SOD1 intensity is displayed in a line graph below each blot. (C) Profiles of SOD1 expression in three MEF cell lines are summarized and depicted in the histogram. The line marks are the same as those described in the Figs. 1 and 2 legend. Data are presented as means ± SEM from three independent experiments [Student's *t* test, * and **, $P < 0.05$].

4. Discussion

Organisms are influenced by their environment and display various rhythms that are governed by a circadian clock, which is self-sustainable and free-running in the region of the brain called the SCN [1–3]. Since an important role for the circadian clock is to enable diverse physiological and biochemical phenomenon to occur at proper times in response to daily environmental changes, it is reasonable to infer that antioxidant enzymes exhibit a daily cycle in their expression. In this study, we explored whether the circadian clock impacts the expression of downstream genes, focusing on *SOD1*. To our knowledge, the regulation of SOD1 expression in circadian mutant mice has not been thoroughly investigated in prior studies. We demonstrated that there are clear differences in the level of expression, enzyme activity, and in the rhythmicity and the phase of the rhythm among mouse genotypes.

Based on our findings, the total amount and enzyme activity of SOD1 in WT mice has a similar pattern to its mRNA levels, with a peak shown at ZT9, implying that SOD1 expression is mainly regulated by transcription. However, in the P2K mutant, both the amount and activity of SOD1 was phase-delayed by 4 h compared to WT mice. The expression pattern of SOD1 was most drastically different in DKO mice, peaking at the late dark phase. Therefore, it appears that WT mice equipped with a normal clock are able to anticipate and prepare countermeasures for the upcoming activity span and accompanying oxidative stresses. In contrast, mutant mice became more sensitive to oxidant stress due to the partial or total breakdown of their circadian clock, which might disrupt the functioning of antioxidant defense mechanisms in these mice.

Most organisms are thought to have antioxidant defense mechanisms that are protective against oxidative stresses originating primarily from metabolic activity and exercise [14]. Several studies have shown that antioxidant defense systems such as free radical scavengers and antioxidant enzymes (e.g., SOD1, catalase, GPx1, and glutathione reductase) are under the influence of circadian rhythms [13–15]. For example, in the rat heart and cerebral cortex, there is a day-night rhythm of lipid peroxidation, and GPx1 and superoxide dismutase activity that appears to be related to modulation of cellular functions [19]. We have also shown the cyclic expression of *SOD1* mRNA in the brain from WT compared to *per*1 knockout mice through *in situ* hybridization [20]. Consistent with our WT data, in most cases, there is an up-regulation of antioxidant defense measures during the nighttime when the ROS level is increased by food intake and exercise.

As mentioned earlier, one cause of oxidant stress is activity. Many animals, including humans, have distinctive patterns of sleep and activity related to daily cycles that lead to definite rhythms in the activities of skeletal muscle and the brain. Through these activities, oxidative stress inducers may manifest time-of-day specific rhythmicity [21,22]. As shown in Fig 3, SOD1 enzyme activities in WT and mutant mice had similar rhythm patterns relating to their mRNA levels. In independent experiments, we could observe that the temporal expression of GPx1 exhibited a very similar pattern to SOD1 in the liver from WT mice and revealed a rhythmic pattern with a peak at ZT9 in WT mice (data not shown). GPx1 acts against oxygen free radicals generated in the presence of peroxides by reducing hydrogen peroxide and lipid peroxides through the oxidation of glutathione [23]. In P2K mice, GPx1 levels did not have

a rhythmic pattern and expression was low. Interestingly, the expression level of GPx1 in DKO mice was the highest among genotypes, but no temporal oscillation patterns were seen, implying that the sensitivity to oxidant stress in these mice was enhanced. At this time, we cannot rule out the possibility that organisms allocate the specific function of individual *per* genes to manage oxidative stresses.

By performing *in vitro* experiments using MEF cell lines, we found a strong correlation between SOD1 level and cell viability, corresponding to the existence of *per* genes when oxidant stress was applied. When we treated cells with a pro-oxidant, *t*-BHP, at a concentration greater than 250 μM, cell viabilities of all 3 MEF cell lines were dramatically decreased up to 50%. We found that the expression of SOD1 gradually increased in a dose-dependent manner in WT and P2K MEF cells. Importantly, the expression of SOD1 in DKO MEF cells was constantly high regardless of the concentration of *t*-BHP added. Because melatonin is known as an effective antioxidant and anticancer agent and is under circadian clock regulation, melatonin may be one possible candidate for mediating SOD1 action against *t*-BHP. There are precedents for the stimulatory action of melatonin on the antioxidant enzyme activities [24,25]. Therefore, the circadian clock may exploit melatonin to allow the defense system to work at the level of expression and activity of antioxidant enzymes such as SOD1 and GPx1.

In summary, the fact that the expression and activity of antioxidant enzymes such as SOD1 are intimately responsive to oxidative stress in both mice and MEF cell lines led us to conclude that the circadian clock gene (*per*) mutants were more influenced by oxidant stress than the control genotype. Further study is required to determine if a connection exists between SOD1 and other clock genes and to ascertain how different antioxidant enzymes are involved in defense mechanisms relating to specific times of the day.

Acknowledgments

The authors thank Dr. Isaac Edery and Dr. Tack-Joong Kim for critical comments on the manuscript. This work was supported by a grant from the National Research Foundation of Korea (NRF) funded by the Korean government (MEST) to K. Bae (No. 2010-0016262).

Appendix A. Supplementary data

Supplementary data associated with this article can be found, in the online version, at doi:10.1016/j.bbrc.2011.04.099.

References

[1] R.Y. Moore, Circadian rhythms: basic neurobiology and clinical applications, Annu. Rev. Med. 48 (1997) 253–266.
[2] J.C. Dunlap, Molecular bases for circadian clocks, Cell 96 (1999) 271–290.
[3] S.M. Reppert, D.R. Weaver, Molecular analysis of mammalian circadian rhythms, Annu. Rev. Physiol. 63 (2001) 647–676.
[4] R.J. Konopka, S. Benzer, Clock mutants of *Drosophila melanogaters*, Proc. Natl. Acad. Sci. USA 68 (1971) 2112–2116.
[5] K. Bae, C. Lee, D. Sidote, K.Y. Chuang, I. Edery, Circadian regulation of a Drosophila homolog of the mammalian Clock gene: PER and TIM function as positive regulators, Mol. Cell. Biol. 10 (1998) 6142–6151.
[6] A. Sehgal, J.L. Price, B. Man, M.W. Young, Loss of circadian behavioral rhythms and per RNA oscillations in the Drosophila mutant timeless, Science 263 (1994) 1603–1606.
[7] I. Edery, Role of posttranscriptional regulation in circadian clock: lessons from *Drosophila*, Chronobiol. Int. 16 (1999) 377–414.
[8] S. Panda, J.B. Hogenesch, S.A. Kay, Circadian rhythms from flies to human, Nature 41 (2002) 329–335.
[9] M.J. Zylka, L.P. Shearman, D.R. Weaver, S.M. Reppert, Three *period* homologs in mammals: differential light responses in the suprachiasmatic circadian clock and oscillating transcripts outside of brain, Neuron 20 (1998) 1103–1110.
[10] F. Makrantonaki, C.C. Zouboulis, Molecular mechanisms of skin aging: state of the art, Ann. N. Y. Acad. Sci. 1119 (2007) 40–50.
[11] M.T. Lin, M.F. Beal, Mitochondrial dysfunction and oxidative stress in neurodegenerative diseases, Nature 443 (2006) 787–795.
[12] G.N. Landis, J. Tower, Superoxide dismutase evolution and life span regulation, Mech. Ageing Dev. 126 (2005) 365–379.
[13] V.C. Culotta, M. Yang, T.V. O'Halloran, Activation of superoxide dismutases: putting the metal to the pedal, Biochim. Biophys. Acta 1763 (2006) 747–758.
[14] R. Hardeland, A. Coto-Montes, B. Poeggeler, Circadian rhythms, oxidative stress, and antioxidative defense mechanisms, Chronobiol. Int. 20 (2003) 921–962.
[15] U. Hodoglugil, O. Ongun, Z. Guney, N. Altan, H. Zengil, Temporal variation in hepatic superoxide dismutase activity in mice, Chronobiol. Int. 12 (1995) 152–155.
[16] V. Jimenez-Ortega, D.P. Cardinali, M.P. Fernandez-Mateos, M.J. Rios-Lugo, P.A. Scacchi, A.I. Esquifino, Effect of cadmium on 24-hour pattern in expression of redox enzyme and clock genes in rat medial basal hypothalamus, Biometals 23 (2010) 327–337.
[17] K. Bae, X. Jin, E.S. Maywood, M.H. Hastings, S.M. Reppert, D.R. Weaver, Differential functions of mPer1, mPer2, and mPer3 in the SCN circadian clock, Neuron 30 (2001) 525–536.
[18] K.J. Livak, T.D. Schmittgen, Analysis of relative gene expression data using real-time quantitative PCR and the 2(-delta delta C(T)) method, Methods 25 (2001) 402–408.
[19] D. Lapenna, S. De Gioia, A. Mezzetti, E. Porreca, G. Ciofani, L. Marzio, F. Capani, C. Di llio, F. Cuccurullo, Circadian variations in antioxidant defences and lipid peroxidation in the rat heart, Free Radic. Res. Commun. 17 (1992) 187–194.
[20] H.G. Kim, Effect of *mPer1* on the expression of *Mup2*, *Cu-Zn SOD* and *HSP105* genes in the SCN, (2006) Yonsei University Press.
[21] D.M. Bailey, B. Davies, I.S. Young, M.J. Jackson, G.W. Davison, R. Isaacson, R.S. Richardson, EPR spectroscopic detection of free radical outflow from an isolated muscle bed in exercising humans, J. Appl. Physiol. 94 (2003) 1714–1718.
[22] C.E. Cooper, N.B. Vollaard, T. Choueiri, M.T. Wilson, Exercise, free radicals and oxidative stress, Biochem. Soc. Trans. 30 (2002) 280–285.
[23] X.G. Lei, W.H. Cheng, J.P. McClung, Metabolic regulation and function of glutathione peroxidase-1, Annu. Rev. Nutr. 27 (2007) 41–61.
[24] R. Hardeland, Antioxidative protection by melatonin: multiplicity of mechanisms from radical detoxification to radical avoidance, Endocrine 27 (2005) 119–130.
[25] S.I. Choi, S. Dadakhujaev, H, Ryu, T. Im Kim, E.K. Kim, Melatonin protects against oxidative stress in granular corneal dystrophy type 2 corneal fibroblasts by mechanisms that involve membrane melatonin receptors, J. Pineal. Res. (2011) doi:10.1111/j.1600-079X.2011.00866.x.